Submitted to small NANO MICRO

DOI: 10.1002/smll.201102156

DNA Length Dependent Fluorescence Signaling on Graphene Oxide Surface**

*Po-Jung Jimmy Huang and Juewen Liu**

[*] Prof. J. L. Corresponding-Author, P.J.H.
Department of Chemistry, Waterloo Institute for Nanotechnology, University of Waterloo, 200 University Avenue West, Waterloo, Ontario, N2L 3G1, Canada
E-mail: liujw@uwaterloo.ca

Supporting Information is available on the WWW under http://www.small-journal.com or from the author.

Keywords: graphene, fluorescence, FRET, DNA, quenching

Graphene has attracted an immense amount of research interest due to its unique electrical, mechanical, optical, and surface properties.[1-4] In addition, with its superior fluorescence quenching and adsorption capacity, graphene has been increasingly used for making biosensors,[5-8] drug delivery vehicles,[9, 10] and imaging agents.[10, 11] To disperse in an aqueous solution, graphene oxide (GO) with surface carboxyl and hydroxyl groups is often prepared. GO is also an excellent quencher for adsorbed fluorophores with quenching efficiency approaching 100%.[12-14] At the same time, GO selectively adsorbs non-structured and single-stranded DNA (ssDNA),[15, 16] which can subsequently desorb upon forming double-stranded (dsDNA) or well-folded structures. Based on these understandings, many optical sensors have been designed for the detection of metal ions,[12, 17, 18] small molecules,[11, 19, 20] proteins,[14, 21] and nucleic acids.[6, 13, 22-24] For example, adsorption of a fluorophorelabeled probe DNA resulted in quenched fluorescence. In the presence of its complementary DNA (cDNA), the fluorescence was recovered due to duplex formation and subsequent desorption. In this

process, the fluorophore-to-GO distance increased from zero to infinity to achieve the maximal fluorescence enhancement. In addition to GO, many other carbon based nanomaterials including carbon nanotubes,[25-29] mesoporous carbon,[30] carbon nanoparticles[31, 32] and water soluble nano-C_{60}[33] have also been tested for similar applications.

On the other hand, little is known about DNA length-dependent fluorescence quenching within a few nanometers from the GO surface. Such information is important for rational design of covalently linked probes. Compared to physisorbed probes, covalent sensors are reversible, regenerable, less prone to non-specific probe displacement, and allow continuous monitoring under flow conditions.[34] In addition, studying distance-dependent fluorescence properties are crucial for the fundamental understanding of DNA/GO interaction and its quenching mechanism. Theoretical calculations predicted that quenching by graphene follows a d^{-4} dependency, where d is the fluorophore-to-graphene distance.[35, 36] This is formally similar to the so-called nanosurface energy transfer (NSET) studied using gold nanoparticles as quencher.[37-40] Seo and co-workers recently measured the fluorescence intensity of Cy3.5 nearby GO separated by up to 18 base pairs (bp) of DNA, where immobilization was achieved via adsorption of a five-adenine overhang.[41]

For a systematic study, we employed eight amino and 6-carboxyfluorescein (FAM) dual-labeled DNAs with varying FAM positions (see Figure 1D for the DNA sequences). The DNAs were respectively reacted with GO in the presence of EDC to form covalent amide linkages (**Figure 1A**, step 1), such that the FAM and GO were separated by 4 to 70 bp. TEM characterization showed that the GO size ranged from a few hundred nanometers to several

micrometers; both single-layered (Figure 1B) and multi-layered (Figure 1C) sheets were present. With the maximal DNA length being ~24 nm in this study, GO can be treated as a large and flat surface for DNA immobilization.

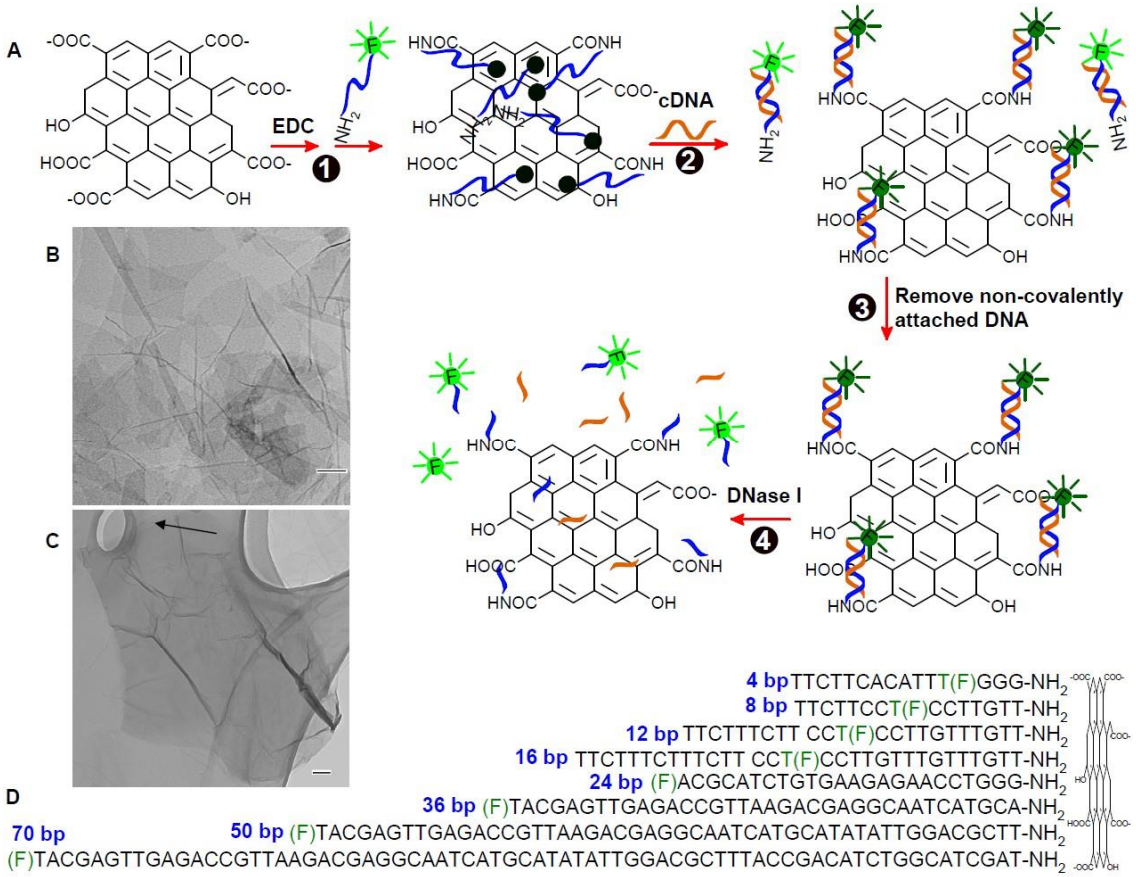

Figure 1. (A) Schematics of the experiment procedure. Step 1: amino and FAMmodified DNAs were conjugated to GO using EDC as the coupling agent. Some DNAs were covalently linked while others were physisorbed; Step 2: addition of the cDNAs resulted in duplex formation; Step 3: the physisorbed DNAs were desorbed and removed. The fluorescence properties of the GO samples containing only covalently attached DNAs were analyzed; Step 4: the total fluorescence was recovered after treating with DNase I. (B, C) TEM micrographs of the GO sheets used in this work. Scale bar = 100 nm. (C) shows the presence of multi-layered GO. The arrow highlights the edge of three graphene layers. (D) The

sequence (from 5′ to 3′) of the eight DNAs used in this study. FAM was denoted as (F) and the internal FAM on a thymine base was denoted as T(F). The amino modifications were on the 3′-end. The number of base pairs separating FAM and amino group was also marked for each DNA.

After the EDC coupling reaction, the GO samples were centrifuged and washed with water to remove the free DNA in the supernatant. The purified GO/DNA complexes were then dispersed and analyzed using steady-state fluorescence spectroscopy. The emission intensities at 520 nm were plotted as a function of the FAM position. As shown in Figure 2B (blue squares), this background fluorescence was close to zero for all eight samples. We found that washing in water was insufficient to completely remove physisorbed DNAs. Therefore, the DNA associated with GO at this moment can be divided into two populations: chemisorbed through the amide bond and physisorbed through hydrophobic interactions. The low background fluorescence indicated that both populations were tightly adsorbed to result in a very short FAM-to-GO distance.

After addition of cDNA, the physisorbed DNAs desorbed upon forming duplexes and the covalently attached ones remained on the surface with their conformation being a rigid rod (Figure 1A, step 2). Using this method physisorbed DNAs were removed after centrifugation (Figure 1A, step 3). In the end, only dsDNA covalently linked to GO remained and a set of representative spectra are shown in **Figure 2A**. For quantitative comparison, the 520 nm peak intensities are plotted in Figure 2B (green dots). The overall trend was that the longer the FAM-to-GO distance, the higher the fluorescence intensity, which suggested that GO acted as an energy acceptor to quench FAM in a distance-dependent manner. By comparing the fluorescence before and after adding cDNA, the signal increase ranged from ~4-fold for the 412 bp samples to >10-fold for the 16-70 bp ones. Therefore, to achieve a good signal-

tobackground ratio, the final FAM-to-GO distance should be greater than 12 bp. Similar observations have been made using fluorescence microscopy and the reaction steps described in Figure 1A have also been followed by fluorescence anisotropy measurement (see Supporting Information, Figure S1, S2).

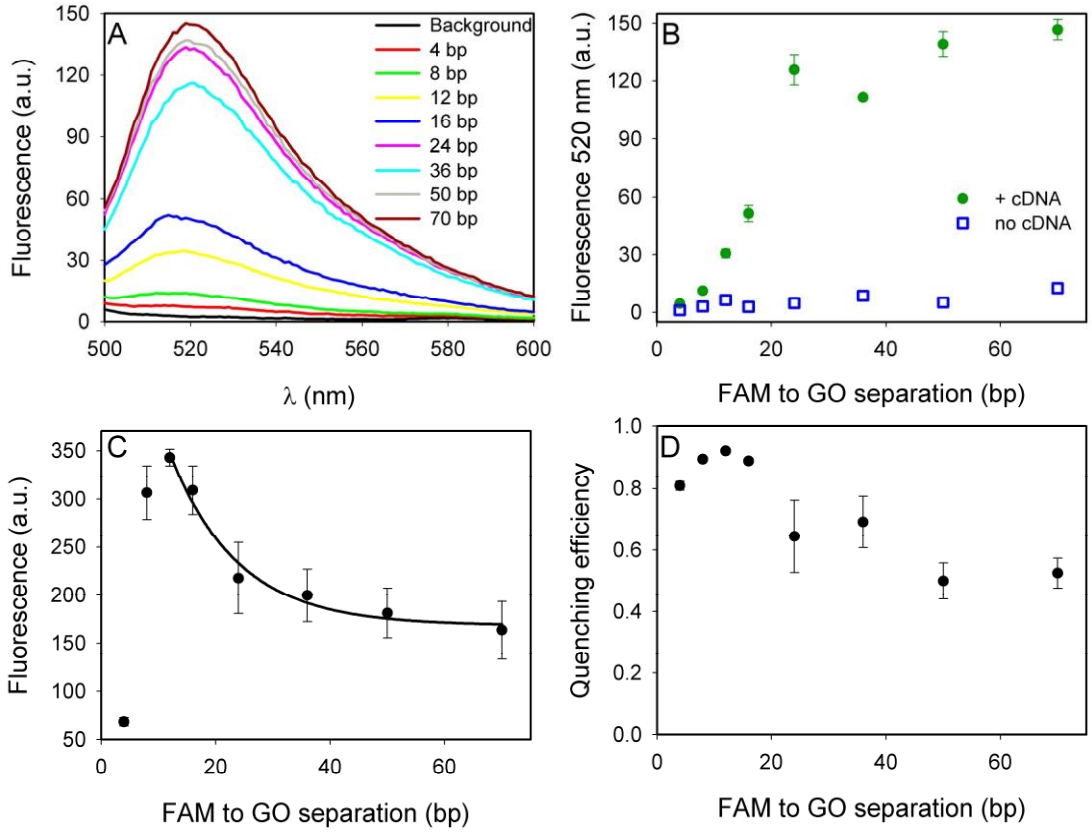

Figure 2. (A) Steady-state fluorescence spectra of the covalently linked dsDNA in buffer A (100 mM NaCl and 25 mM HEPES, pH 7.6). (B) The 520 nm peak intensity as a function of the FAM position before (squares) and after (dots) addition of cDNA. (C) Fluorescence intensity of the immobilized dsDNA samples after DNase I treatment. (D) Quenching efficiency of the immobilized dsDNA as a function of the FAM position.

While DNA length-dependent signaling was demonstrated in Figure 2B, few quantitative conclusions can be drawn since the observed fluorescence intensity was also

influenced by other factors such as the coupling efficiency or DNA density on GO. In addition, the exact quenching efficiency for each sample can be obtained only after knowing the fluorescence intensity of the same sample with an infinite FAM-to-GO distance. To answer these questions, DNase I was added in order to cleave the DNA and release FAM (Figure 1A, step 4). As shown in Figure 2C, the fluorescence after the DNase treatment was very low for the 4 bp sample followed by a sharp increase for the 8 bp DNA and then a gradual decay starting from the 12 bp sample. The data from 12 to 70 bp were fit to an exponential decay curve and this decay trend reflected the coupling efficiency of the EDC reaction. Our result indicated that longer DNA had a lower coupling efficiency under otherwise identical conditions, which was attributed to the slower diffusion and shielding of the amino group by the longer DNA chains. Following this trend, the highest fluorescence should have been the 4 bp sample. The fact that both the 4 and 8 bp DNA had low fluorescence suggests that the DNase activity may be impeded close to the GO surface.

With the DNase data, we were able to determine the quenching efficiency $Q = 1-F_C/F_E$, where F_C was the fluorescence after cDNA addition and F_E was after the further addition of DNase. As shown in Figure 2D, quenching was ~90% for the short DNA chains and was progressively decreased for the longer ones. The 4 and 8 bp samples showed lower quenching efficiency than that for the 12 bp DNA, which was related to the compromised DNase activity as discussed previously. Interestingly, ~50% quenching was still observed even for the 70 bp sample with a FAM-to-GO distance of ~24 nm. In fluorescence energy transfer, the characteristic fluorophore-to-quencher distance for 50% quenching is called the Förster distance. Although energy transfer to GO is unlikely to be through the Förster mechanism,[42] the concept of this characteristic distance still applies. For example, theoretic calculations showed that for graphene, $Q = 1/[1+(d/d_0)^4]$, where d_0 was the characteristic distance and d

was the fluorophore-to-GO distance. d_0 was estimated to be ~5 nm between a conjugated polymer and GO.[43] In another system, although not explicitly reported, d_0 can be estimated to be ~6.8 nm for the FAM/GO pair, since GO can quench 68% fluorescence within 10 nm (see Supporting Information for the estimation).[44, 45] By comparing our results with the literature values, we reasoned that either a portion of the DNA was not aligned vertically with respect to the GO surface or multi-layered GO being better quenchers must be taken into account.[44] Because of this uncertainty, we cannot calculate the characteristic distance for the FAM/GO pair at this moment.

Steady-state fluorescence provided information about the total quenching, which contained both static and dynamic components, where static quenching involved a very short FAM-to-GO distance and possibly ground state complex formation. The dynamic quenching component can be extracted from fluorescence lifetime measurement. Such studies can also provide information about different quenching environments that a fluorophore might be in. As shown in **Figure 3A**, a FAM-labeled DNA freely dispersed in solution (no GO) had a single exponential decay with a lifetime of 4.05 ns. After incubating the GO samples with cDNA, the lifetime decay traces were also collected. All these samples decayed faster than the free DNA, confirming the contribution of dynamic quenching caused by GO. It can also be observed that none of the GO samples followed single exponential decay, indicating the presence of different quenching environments.

The lifetime decay traces were fitted using a double exponential decay model (**Table 1**) and the average lifetime was calculated. The quenching efficiency was obtained using $Q = 1-\tau/\tau_0$, where τ was the average lifetime in the presence of GO,[42] and τ_0 = 4.05 ns, the lifetime in the absence of GO. The quenching efficiency obtained from lifetime was plotted in Figure 3B (squares), and as expected, it decreased with increasing DNA length. For

comparison, the total quenching is also presented in the same figure (dots, re-plotted from Figure 2D). Therefore, for all of the DNAs, the main quenching mechanism was dynamic quenching, since the static quenching component was the difference between these two, which was less than 10% for most of the samples. This experiment suggested that most of the FAMs were not closely adsorbed after forming the dsDNA.

The fact that fluorescence lifetime did not follow a single exponential decay indicated the presence of different quenching environments, which could be related to the presence of multi-layered GO, the different orientations of the DNA on GO, or DNA dynamics. The orientation of DNA on graphene has been studied by computer modeling and it was found that dsDNA can either sit vertically on the surface via □□-stacking or horizontally with the end base pairs open to interact with the surface.[46] These adsorbed DNA were stable for at least several tens of ns (the maximal time used for the simulation), which was much longer compared to the excited lifetime of FAM. Therefore, the dynamics of DNA was unlikely to be the reason for the observed multi-exponential lifetime decay.

If we consider the presence of stably-adsorbed DNA with both vertical and horizontal alignments, the vertical DNA should show a length-dependent lifetime change; while horizontal ones should be drastically quenched independently from its length since the FAMto-GO distance should be equal to or shorter than the DNA diameter of just 2 nm. If we take the characteristic distance to be 7.5 nm (*vide infra*), FAM from horizontal DNA should show a lifetime of shorter than 0.02 ns, which is below the detection limit of our instrument, and can be considered to be effectively static quenching. As a result, we need only to consider the vertically-aligned DNA for the purpose of assigning fluorescence lifetime. In addition, the population of horizontally-aligned DNA must be quite low due to the electrostatic repulsion between the DNA backbone and GO surface (note that the simulation work was performed

using graphene instead of GO)[46] and the vertical alignment should be electrostatically favored. This hypothesis was supported by the fact that very little static quenching was observed for all the samples. Therefore, DNA orientation cannot explain the non-single exponential lifetime decay either and we propose that the presence of multi-layered GO sheets to be the main reason.

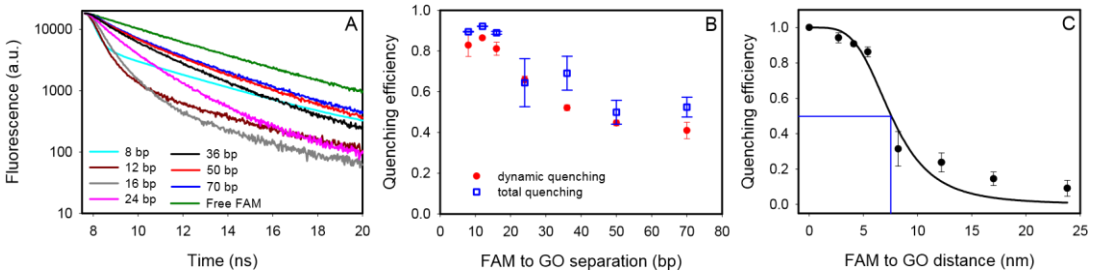

Figure 3. (A) Time domain fluorescence lifetime decay traces of the covalently linked FAMlabeled DNA after forming duplex with cDNA. (B) Quenching efficiency plotted as a function of the FAM-to-GO separation calculated based on the average fluorescence lifetime (dots) and from steady-state fluorescence (squares), which was the same as Figure 2D. (C) Quenching efficiency (from lifetime fitting) as a function of FAM-to-GO distance on singlelayered GO. The data were fit using $Q = 1/[1+(d/d_0)^4]$ and d_0 corresponding to 50% quenching is marked.

Table 1. Results of fluorescence lifetime decay fitting into a double exponential model. A_1 and A_2 are the respective percentage for lifetime τ_1 and τ_2. The average τ is calculated using the equation $\tau = (A_1 \tau_1 + A_2 \tau_2)/(A_1 + A_2)$. The numbers in boldface were considered to be from single-layered GO and were used for data fitting in Figure 3C.

FAM-GO (bp)	FAM-GO (nm)	A1 (%)	τ1 (ns)	A2 (%)	τ2 (ns)	Average τ (ns)
8	2.7	**90 ± 5**	**0.24 ± 0.11**	10 ± 5	3.88 ± 0.05	0.59
12	4.1	**95 ± 2**	**0.37 ± 0.05**	5 ± 2	3.62 ± 0.07	0.55
16	5.4	**93 ± 3**	**0.56 ± 0.11**	7 ± 3	3.18 ± 0.30	0.75
24	8.2	78 ± 3	0.88 ± 0.20	**22 ± 3**	**2.78 ± 0.40**	1.30
36	12.2	61 ± 3	0.90 ± 0.28	**39 ± 2**	**3.09 ± 0.22**	1.76
50	17	57 ± 3	0.96 ± 0.30	**43 ± 3**	**3.46 ± 0.16**	2.03
70	23.8	57 ± 4	0.99 ± 0.31	**43 ± 4**	**3.68 ± 0.18**	2.14

The lifetime fitting using a double exponential model is presented in **Table 1**. The 4 bp sample was not included since its overall quantum yield was close to zero and its lifetime cannot be accurately measured. For the 8 to 16 bp samples, the major population (>90%) had a very short lifetime of 0.2-0.6 ns. The vertical distance between GO and FAM was only 5.4 nm even for the 16 bp sample, which should result in a lifetime of ~0.8 ns (calculated based on d = 5.4 nm and d_0 = 7.5 nm for single-layered GO). The fact that the 16 bp sample had a lifetime component of ~0.6 ns suggested that most of its lifetime signal was from vertically aligned DNA on single-layered GO. Multi-layered GO had a larger d_0 value since they were better quenchers. With the d^{-4} dependence on quenching efficiency, the lifetime contribution from multi-layered GO for the shorter DNA samples (e.g. 8 and 12 bp) should be even smaller. Therefore, for these three samples, the short lifetime components were mainly from the single-layered GO. We also obtained a minor population (< 10%) with long lifetime (e.g. close to the free FAM lifetime of 4 ns), suggesting the presence of large GO domains or sheets that were poor quenchers, possibly due to a high level of oxidation. The area of such sheets should be < 10% of the total GO surface area.

To further understand quenching, we performed fluorescence lifetime imaging microscopy (FLIM) experiments (see Supporting Information). Figure S3A shows the spatial

lifetime distribution of the 16 bp sample, where most of the areas showed a lifetime of ~0.5 ns (Figure S3B), consistent with the lifetime spectroscopy data in Table 1. A number of long lifetime regions were also observed on these GO sheets. Therefore, it should be appropriate to fit these short DNAs into a double exponential decay model.

For the longer DNAs (36-70 bp), the long lifetime population reached 40-45% with lifetime progressively approaching 4 ns. Since only less than 10% can be attributed to the highly oxidized surface, the remaining >30% must be due to the increased FAM-to-GO distance. These DNA chains had a vertical FAM-to-GO distance greater than 12.2 nm (i.e. for the 36 bp sample). Assuming d_0 = 7.5 nm, a 12.2 nm separation should give a lifetime of ~3.4 ns, which is close to the 3.1 ns obtained from fitting. Therefore, we assigned these long lifetime component to the vertically-aligned DNA on single-layered GO. The only sample left was the 24-bp chain with a vertical FAM-to-GO distance of 8.2 nm. According to the fitting, it has 78% of 0.98 ns and 22% of 2.59 ns. Since 22% is also significantly more than 10%, we consider that the 2.59 ns population to be vertically aligned on single-layered GO. This length was close to the critical distance and a large variation in quenching efficiency was expected with small distance changes, which may contribute to the large error bar size for this sample. Based on the above discussion, we plotted the quenching efficiency of single-layered GO as a function of distance and fit the data using $Q = 1/[1+(d/d_0)^4]$ (Figure 3C). The characteristic distance d_0 was calculated to be 7.5 ± 0.6 nm, which agreed well with the estimated ~6.8 nm from other experiments.[44] It was reported that d_0 for the FAM/gold nanoparticle pair was 7.6 nm, which also followed the d^{-4} dependency,[37, 38, 40] although the mechanism of quenching by metallic gold is inherently different from quenching by the planar carbon π system.

For the long DNA samples, about half of the population showed a lifetime of ~0.8-1 ns, which corresponded to a FAM-to-GO distance of ~5.5 nm on single-layered GO. This

would require the DNAs to tilt with an angle of 14° for the 70 bp sample and 30° for the 36 bp one. However, there was no particular intermolecular force to justify such angles and theoretical calculations only supported the vertical and horizontal alignments. To further understand this, we performed FLIM experiments also on the 70 bp sample (see Supporting Information, Figure S3C), where domains of a few μm with different lifetimes were observed. These domain sizes agreed with the size of individual GO sheets and therefore its lifetime distribution was likely to be due to the different quenching ability of different sheets, suggesting the effect of multilayered GO. It is known that quenching is significantly enhanced with increasing number of GO layers.[44] GO preparation using chemical exfoliation generates not only single but also multiple layers,[47, 48] which were observed in the TEM micrographs in Figure 1C. For the long DNAs, fitting with a double exponential model can be justified only when the quenching by all of the multi-layered GO was significantly higher than that by the single-layered. However, the limited information content from the lifetime experiment did not allow us to consider all the different layered samples, which could be one of the error sources for the characteristic energy transfer distance measurement in Figure 3C.

In summary, we identified three DNA populations on GO surface. Those immobilized on highly oxidized domains should count for no more than 10% of the DNA. The immobilized FAM on these dsDNA was barely quenched to show a lifetime of ~4 ns. The second population was on the normal single-layered GO sheets and this population should be close to 40% in our samples. Finally, there were also DNAs on multi-layered GO sheets. For these samples, the range of quenching was much longer. During our sample preparation, six centrifugation steps were carried out before the lifetime measurement. This was likely to decrease single-layered GO and accumulate high density multi-layers, contributing to their abundance in the lifetime experiment. All the major fluorescence signaling techniques have been tested in this work on

these covalently immobilized DNA probes and this study supports the use of such probes for analytical and biomedical applications.

Experimental Section

Chemicals: All DNA samples were purchased from Integrated DNA Technologies (Coralville, IA). The FAM and amino labeled DNA sequences and modifications are listed in Figure 1D. Sodium chloride, magnesium chloride, 4-Morpholineethanesulfonate (MES) and 4-(2hydroxyethyl)piperazine-1-ethanesulfonate (HEPES) were purchased from Mandel Scientific (Guelph, Ontario, Canada). *N*-(3-Dimethylaminopropyl)-*N′*-ethylcarbodiimide hydrochloride (EDC) was purchased from Sigma-Aldrich. DNase I was purchased from VWR. GO was prepared as described previously and supplied by our collaborator.[16]

Covalent attaching DNA to GO: The conjugation reaction was carried out in a glass vial with a final volume of 500 μL containing 100 μg/mL GO, 2 μM amino-modified DNA, 10 mM EDC (freshly prepared), 25 mM NaCl and 25 mM MES, pH 6.0. The reaction was allowed for 3 hr at room temperature under magnetic stirring. The GO/DNA conjugates were purified by centrifugation at 15000 rpm for 20 min followed by removal of the supernatant. The GO/DNA conjugates were then washed with 500 μL of water twice to further remove nonassociated DNAs. Finally, the conjugates were dispersed in buffer A (25 mM HEPES, pH 7.6, 100 mM NaCl) with a final GO concentration of 100 μg/mL and stored at 4 °C before use.

Forming dsDNA on GO. To form dsDNA on GO, 4 μM the cDNAs were respectively added to the above-prepared GO samples. After overnight incubation, the samples were centrifuged at 15000 rpm for 20 min and the supernatant was carefully removed. Another 4 μM cDNA was added and this process was repeated three times to ensure that all the physisorbed DNAs were removed and only covalently attached dsDNAs were left on the surface. To release FAM

from DNA on the GO surface, 25 U of DNase I was added to each of the 50 μL GO sample (in 40 mM Tris HCl, pH 8.0, 10 mM $CaCl_2$, and 5 mM $MgCl_2$). The samples were then incubated at 35 °C for 15 min and then at room temperature for 1 hr.

Steady-state fluorescence spectra. Steady state fluorescence spectra were collected using a Varian Eclipse spectrofluorometer. The excitation wavelength was set at 485 nm and the emission spectra from 500 to 600 nm were collected. The GO concentration in the cuvette was 20 μg/mL.

Fluorescence anisotropy. All eight DNA samples were analyzed using fluorescence anisotropy. The experiment was carried out on a Molecular Device M5 fluorescence microplate reader. For measurements without GO, each well contained 100 nM of the free ssDNA or dsDNA. For immobilized dsDNA, a GO concentration of 20 μg/mL GO was used and the buffer contained 150 mM NaCl, 25 mM HEPES, and 1mM $MgCl_2$. The excitation wavelength was set to be 485 nm and emission at 520 nm was monitored. A g-factor of 1.095 was used for all the samples.

Fluorescence lifetime spectroscopy. 400 μL of 20 μg/mL GO sample were loaded into a quartz micro-cuvette for lifetime measurement. Fluorescence lifetime was collected using PicoQuant FluoTime 100 spectrofluorometer. The laser light source at 470 nm was used for the excitation. A 520 nm band pass filter was applied on the emission side. The data were fitted to a double exponential decay.

Fluorescence microscopy. The GO samples were observed using Leica DMI 3000B inverted microscope with a Hamamatsu ORCA-R^2 camera system. The GO samples were concentrated to ~200 μg/mL with 2 μL being spotted on a glass slide. The samples were imaged after putting on a cover slip. The cube for green fluorescence imaging was used. The fluorescence microscopy images were taken under the 40× objective with an exposure time of 10 sec.

Fluorescence lifetime imaging. The fluorescence lifetime images were captured using Leica DM 6000B microscope with Leica TCS SP5 system using the 63× (glycerol) objective. The excitation source was a multiphoton IR laser.

*TEM***.** The TEM micrographs were acquired on a Philips CM10 transmission electron microscope. The GO samples (0.2 mg/mL) were dropped on a holey carbon TEM grid for imaging.

Acknowledgements

We thank Dr. Michael Palmer at the University of Waterloo for help with fluorescence lifetime spectroscopy and stimulating discussions and Dr. Michaela Strüder-Kypke at the University of Guelph for assistance with fluorescence lifetime imaging. IR was carried out with the assistance of Dr. L. Zhang. The GO samples were provided by Ravindra Kempaiah and Vivek Maheshwari. Funding for this work is from the University of Waterloo, the Canadian Foundation for Innovation, and the Discovery Grant of the Natural Sciences and Engineering Research Council (NSERC) of Canada. J. Liu receives Early Researcher Award from the Ontario Ministry of Research and Innovation.

[1] A. K. Geim, K. S. Novoselov, *Nat. Mater.* **2007**, *6*, 183.

[2] M. J. Allen, V. C. Tung, R. B. Kaner, *Chem. Rev.* **2009**, *110*, 132.

[3] C. N. R. Rao, A. K. Sood, K. S. Subrahmanyam, A. Govindaraj, *Angew. Chem. Int. Ed.* **2009**, *48*, 7752.

[4] K. P. Loh, Q. Bao, G. Eda, M. Chhowalla, *Nat Chem* **2010**, *2*, 1015.

[5] W. R. Yang, K. R. Ratinac, S. P. Ringer, P. Thordarson, J. J. Gooding, F. Braet, *Angew. Chem. Int. Ed.* **2010**, *49*, 2114.

[6] Y. Y. Shao, J. Wang, H. Wu, J. Liu, I. A. Aksay, Y. H. Lin, *Electroanalysis* **2010**, *22*, 1027.

[7] Y. Wang, Z. H. Li, J. Wang, J. H. Li, Y. H. Lin, *Trends Biotechnol.* **2011**, *29*, 205.

[8] B. Gulbakan, E. Yasun, M. I. Shukoor, Z. Zhu, M. X. You, X. H. Tan, H. Sanchez, D. H. Powell, H. J. Dai, W. H. Tan, *J. Am. Chem. Soc.* **2010**, *132*, 17408.

[9] Z. Liu, J. T. Robinson, X. M. Sun, H. J. Dai, *J. Am. Chem. Soc.* **2008**, *130*, 10876. [10] X. M. Sun, Z. Liu, K. Welsher, J. T. Robinson, A. Goodwin, S. Zaric, H. J. Dai, *Nano Research* **2008**, *1*, 203.

[11] Y. Wang, Z. H. Li, D. H. Hu, C. T. Lin, J. H. Li, Y. H. Lin, *J. Am. Chem. Soc.* **2010**, *132*, 9274.

[12] S. J. He, B. Song, D. Li, C. F. Zhu, W. P. Qi, Y. Q. Wen, L. H. Wang, S. P. Song, H. P. Fang, C. H. Fan, *Adv. Funct. Mater.* **2010**, *20*, 453.

[13] C. H. Lu, H. H. Yang, C. L. Zhu, X. Chen, G. N. Chen, *Angew. Chem. Int. Ed.* **2009**, *48*, 4785.

[14] H. F. Dong, W. C. Gao, F. Yan, H. X. Ji, H. X. Ju, *Anal. Chem.* **2010**, *82*, 5511. [15] B. S. Husale, S. Sahoo, A. Radenovic, F. Traversi, P. Annibale, A. Kis, *Langmuir* **2010**, *26*, 18078.

[16] M. Wu, R. Kempaiah, P.-J. J. Huang, V. Maheshwari, J. Liu, *Langmuir* **2011**, *27*, 2731.

[17] Y. Q. Wen, F. F. Xing, S. J. He, S. P. Song, L. H. Wang, Y. T. Long, D. Li, C. H. Fan, *Chem. Comm.* **2010**, *46*, 2596.

[18] M. Zhang, B.-C. Yin, W. Tan, B.-C. Ye, *Biosens. Bioelectron.* **2011**, *26*, 3260.

[19] C.-H. Lu, J. Li, M.-H. Lin, Y.-W. Wang, H.-H. Yang, X. Chen, G.-N. Chen, *Angew. Chem., Int. Ed.* **2010**, *49*, 8454.

[20] P.-J. J. Huang, R. Kempaiah, J. Liu, *J. Mater. Chem.* **2011**, *21*, 8991.

[21] H. X. Chang, L. H. Tang, Y. Wang, J. H. Jiang, J. H. Li, *Anal. Chem.* **2010**, *82*, 2341.

[22] F. Li, Y. Huang, Q. Yang, Z. T. Zhong, D. Li, L. H. Wang, S. P. Song, C. H. Fan, *Nanoscale* **2010**, *2*, 1021.

[23] C. H. Lu, J. Li, J. J. Liu, H. H. Yang, X. Chen, G. N. Chen, *Chem. Eur. J.* **2010**, *16*, 4889.

[24] W. Wu, H. Hu, F. Li, L. Wang, J. Gao, J. Lu, C. Fan, *Chem. Comm.* **2011**, *47*, 1201.

[25] R. H. Yang, J. Y. Jin, Y. Chen, N. Shao, H. Z. Kang, Z. Xiao, Z. W. Tang, Y. R. Wu, Z. Zhu, W. H. Tan, *J. Am. Chem. Soc.* **2008**, *130*, 8351.

[26] S. J. Zhen, L. Q. Chen, S. J. Xiao, Y. F. Li, P. P. Hu, L. Zhan, L. Peng, E. Q. Song, C. Z. Huang, *Anal. Chem.* **2010**, *82*, 8432.

[27] L. Zhang, H. Wei, J. Li, T. Li, D. Li, Y. Li, E. Wang, *Biosens. Bioelectron.* **2010**, *25*, 1897.

[28] Z. Chen, X. B. Zhang, R. H. Yang, Z. Zhu, Y. Chen, W. H. Tan, *Nanoscale* **2011**, *3*, 1949.

[29] H. Li, J. Tian, L. Wang, Y. Zhang, X. Sun, *J. Mater. Chem.* **2011**, *21*, 824.

[30] S. Liu, H. Li, L. Wang, J. Tian, X. Sun, *J. Mater. Chem.* **2011**, *21*, 339.

[31] H. Li, Y. Zhang, T. Wu, S. Liu, L. Wang, X. Sun, *J. Mater. Chem.* **2011**, *21*, 4663.

[32] H. Li, Y. Zhang, L. Wang, J. Tian, X. Sun, *Chem. Comm.* **2011**, *47*, 961.

[33] H. Li, Y. Zhang, Y. Luo, X. Sun, *Small* **2011**, *7*, 1562.

[34] D. Li, S. P. Song, C. H. Fan, *Acc. Chem. Res.* **2010**, *43*, 631.

[35] R. S. Swathi, K. L. Sebastian, *Journal of Chemical Physics* **2008**, *129*, 9.

[36] R. S. Swathi, K. L. Sebastian, *Journal of Chemical Physics* **2009**, *130*, 3.

[37] C. S. Yun, A. Javier, T. Jennings, M. Fisher, S. Hira, S. Peterson, B. Hopkins, N. O. Reich, G. F. Strouse, *J. Am. Chem. Soc.* **2005**, *127*, 3115.

[38] T. L. Jennings, M. P. Singh, G. F. Strouse, *J. Am. Chem. Soc.* **2006**, *128*, 5462.

[39] T. Sen, A. Patra, *The Journal of Physical Chemistry C* **2008**, *112*, 3216.

[40] Y. Chen, M. B. O'Donoghue, Y. F. Huang, H. Z. Kang, J. A. Phillips, X. L. Chen, M. C. Estevez, C. Y. J. Yang, W. H. Tan, *J. Am. Chem. Soc.* **2010**, *132*, 16559.

[41] Y. Piao, F. Liu, T. S. Seo, *Chem. Comm.* **2011**, *47*, 12149.

[42] R. M. Clegg, *Meth. Enzymol.* **1992**, *211*, 353.

[43] Y. Wang, D. Kurunthu, G. W. Scott, C. J. Bardeen, *The Journal of Physical Chemistry C* **2010**, *114*, 4153.

[44] J. Kim, L. J. Cote, F. Kim, J. Huang, *J. Am. Chem. Soc.* **2010**, *132*, 260.

[45] J. Kim, F. Kim, J. X. Huang, *Materials Today* **2010**, *13*, 28.

[46] X. Zhao, *The Journal of Physical Chemistry C* **2011**, *115*, 6181.

[47] C.-J. Shih, A. Vijayaraghavan, R. Krishnan, R. Sharma, J.-H. Han, M.-H. Ham, Z. Jin, S. Lin, G. L. C. Paulus, N. F. Reuel, Q. H. Wang, D. Blankschtein, M. S. Strano, *Nat Nano* **2011**, *6*, 439.

[48] P. Hasin, M. A. Alpuche-Aviles, Y. Y. Wu, *J. Phys. Chem. C* **2010**, *114*, 15857.

Received: 13 October 2011
Revised: 12 December 2011
Published online on 10 February 2012